Biochimica et Biophysica Acta 1808 (2011) 2646–2655

Contents lists available at ScienceDirect

Biochimica et Biophysica Acta

journal homepage: www.elsevier.com/locate/bbamem

Nanoscale structural and mechanical effects of beta-amyloid (1–42) on polymer cushioned membranes: A combined study by neutron reflectometry and AFM Force Spectroscopy

Silvia Dante [a,b,c,*], Thomas Hauß [a], Roland Steitz [a], Claudio Canale [b], Norbert A. Dencher [d]

[a] Helmholtz Zentrum Berlin für Materialien und Energie, Institute for Soft Matter and Functional Materials, Hahn-Meitner Platz 1, 14109 Berlin, Germany
[b] Nanophysics Unit, Facility of Nanobiotechnology, Italian Institute of Technology, Via Morego 30, 16163 Genova, Italy
[c] Department of Neuroscience and Brain Technology, Italian Institute of Technology, Via Morego 30, 16163 Genova, Italy
[d] Institute of Chemistry, Physical Biochemistry, Technische Universität Darmstadt, Petersenstrasse 22, 64287 Darmstadt, Germany

ARTICLE INFO

Article history:
Received 3 April 2011
Received in revised form 6 July 2011
Accepted 19 July 2011
Available online 24 July 2011

Keywords:
Beta-amyloid
Lipid bilayer
Polymer cushion
Neutron reflectivity
Force spectroscopy

ABSTRACT

The interaction of beta-amyloid peptides with lipid membranes is widely studied as trigger agents in Alzheimer's disease. Their mechanism of action at the molecular level is unknown and their interaction with the neural membrane is crucial to elucidate the onset of the disease. In this study we have investigated the interaction of water soluble forms of beta-amyloid Aβ(1–42) with lipid bilayers supported by polymer cushion. A reproducible protocol for the preparation of a supported phospholipid membrane with composition mimicking the neural membrane and in physiological condition (PBS buffer, pH = 7.4) was refined by neutron reflectivity. The change in structure and local mechanical properties of the membrane in the presence of Aβ(1–42) was investigated by neutron reflectivity and Atomic Force Microscopy (AFM) Force Spectroscopy. Neutron reflectivity evidenced that Aβ(1–42) interacts strongly with the supported membrane, causing a change in the scattering length density profile of the lipid bilayer, and penetrates into the membrane. Concomitantly, the local mechanical properties of the bilayer are deeply modified by the interaction with the peptide as seen by AFM Force Spectroscopy. These results may be of great importance for the onset of the Alzheimer's disease, since a simultaneous change in the structural and mechanical properties of the lipid matrix could influence all membrane based signal cascades.

1. Introduction

The role of beta-amyloids (Aβs) as trigger agents of the neurodegenerative disease known as Alzheimer's disease (AD) is widely recognized [1,2]. Fibril forms of these peptides are the main component of the extracellular amyloid plaques, a hallmark of AD [3]. Recently, the effect of soluble forms of Aβs, like protofibrils or small oligomers, on neural cells has been taken into consideration, since the correlation between symptoms of AD with these small soluble aggregates of Aβ is more pronounced as is the correlation with amyloid plaques [4]. The interaction of soluble forms of Aβs with the neural membrane is essential to elucidate the role of the toxic peptide in the neurodegenerative cascade typical of AD. Aβ(1–42), the most aggressive form of the peptide present in the senile plaques, was shown to be very membrane active and to induce fusion of unilamellar vesicles (ULV) [5]. Moreover, a study by AFM on solid supported double layers [6] showed that this peptide can damage the membrane.

Previous investigations by X-rays and neutron diffraction revealed that the short analogue Aβ(25–35) perturbs the lipid double layer as a function of the membrane charge and composition [7–9]. Aβ(25–35) has an effect on the lateral diffusion of lipids, as recently detected by quasi-elastic neutron scattering (QENS) [10].

We have considered the interaction of water soluble forms of Aβ(1–42) with lipid membranes supported by polymer cushion. Compared to solid supported membranes, membranes supported on polymer cushion are a better model for natural membranes: the introduction of a soft cushion, covalently or non-covalently linked to the support [11–13], decouples the membranes from the solid substrate and retains the membrane's natural fluidity as well as the freedom to deform and to incorporate membrane-spanning peptides

Abbreviations: AD, Alzheimer's disease; Aβ(1–42), β-amyloid (1–42); Aβs, soluble amyloid-beta; APP, amyloid precursor protein; AFM-FS, Atomic Force Microscopy Force Spectroscopy; DLS, dynamic light scattering; NR, neutron reflectivity; PBS, phosphate buffer saline; PAH, polyallylamine hydrochloride; PEI, polyethylenemine; PEM, polyelectrolyte multilayer; PSS, polystyrene sulfonate; POPC, 1-palmitoyl-2-oleoyl-phosphatidylcholine; (POPS), 1-palmitoyl-2-oleoyl-phosphatidyl serine; (POPC-D31), 1-palmitoyl(D31)-2-oleoyl-phosphatidylcholine; POPS-D31, 1-palmitoyl(D31)-2-oleoylphosphatidyl serine; QENS, Quasi Elastic Neutron Scattering; SANS, small-angle-neutron scattering; SLD, scattering length density; SLM, supported lipid membranes; TFA, trifluoroacetic acid; ULV, unilamellar lipid vesicles

* Corresponding author at: Nanophysics Unit, Facility of Nanobiotechnology, Italian Institute of Technology, Via Morego 30, 16163 Genova, Italy. Tel.: +39 010 71781541.
E-mail address: silvia.dante@iit.it (S. Dante).

0005-2736/$ – see front matter © 2011 Elsevier B.V. All rights reserved.
doi:10.1016/j.bbamem.2011.07.024

and proteins. In particular, the use of water swellable polymers allows creating deformable and soft substrate similar to the cytoskeleton of living cells [14,15]. Recently, attention was focused on charged polymeric supports, such as polyelectrolytes prepared by self-assembly, because of the possibility to tune and define the film thickness to the monomolecular level.

We employed as polymer cushion polyelectrolytes deposited layer-by-layer [16]; the supported membrane was obtained by adhesion and subsequent fusion of unilamellar vesicles (ULV) carrying a membrane charge opposite to that of the outermost polyelectrolyte layer of the cushion. The formation of a continuous lipid bilayer requires a balance between the affinity between lipids and support, which governs adhesion, and the mobility of the lipid at the interface. The success of bilayer formation depends on the properties of the interface and of the lipid mixture, as well as on other parameters like concentration, temperature, pH and ionic strength of the solution [17,18]. As demonstrated by neutron reflectivity (NR), we accomplished to have a protocol for reproducible formation of polymer supported membranes in physiological buffer.

NR is a well-established technique for studying membranes at the solid/water interface [19–22]. It provides detailed information on the structure and on the composition of the interface. The composition profile along the z direction, perpendicular to the membrane plane, can be measured with a resolution down to 0.2 nm. NR is based on the variation of specular reflection R at the interface between two materials with the variation of the wave vector transfer $Q=(4\pi/\lambda)\sin\theta$, where λ is the wavelength of the neutron and θ is the incident angle of the neutron beam. The variation of R with Q depends on the composition of the interface, characterized by the scattering length density $SLD(z)=\Sigma n_i b_i/V_i$, where b is the scattering length of the i-th element with number n and volume V composing the interface. In this study, NR was employed to investigate the changes induced on the structure of the lipid bilayers upon interaction with the neurotoxic peptide Aβ(1–42). The information obtained by NR was supported by results from AFM Force Spectroscopy (AFM-FS) on the same system.

Atomic Force Microscopy (AFM) has become a well-established technique for imaging supported lipid membranes (SLBs) at nanometer resolution [23–25]. In the Force Spectroscopy mode, the AFM tip approaches and retracts towards the sample. In these approach–retraction cycles the cantilever deflection is recorded as a function of the piezo vertical displacement to yield the so-called force–distance curves. Recently, FS has become a tool to characterize SLB on solid support. Force–distance curves in the approach direction give information about the breakthrough force for SLBs, a parameter that is directly related to lipid packing and lipid order in the membrane. At a certain force a discontinuity appears in the force–distance curve, which is indicative of the tip penetrating the bilayer and leading to the onset of plastic deformation. In some cases force mapping has been used to create two dimensional adhesion maps from a sequence of force curves [26–28]. We recently proposed a home built algorithm implemented in Matlab, to process a high number of curves from force mapping and capable to extract different physical parameters, i.e., single and multiple breakthrough forces, the yield depth associated to each breakthrough event and the adhesion forces extracted from each curve [29], creating a two-dimensional map for each of these physical parameters.

The information obtained by the two techniques is complementary, since the techniques refer to two perpendicular dimensions of the membrane; moreover, they connect two different aspects of the peptide/membrane interaction, i.e., the structural changes and influence on the mechanical properties of the membrane induced by peptides such as Aβ.

By applying NR and AFM-FS on supported membranes we demonstrated that the AD peptide Aβ(1–42) penetrates the membrane under physiological condition and strongly perturbs its mechanical stability.

Understanding the structural and mechanical properties of the bilayers of different composition at the nano scale will provide us the basis for the interpretation of the interaction of the membrane with exogenous molecules.

2. Material and methods

2.1. Lipids

The phospholipids used for vesicle preparation were the zwitterionic 1-palmitoyl-2-oleoyl-phospatidylcholine (POPC), and its partially deuterated analogue D31-POPC; the negatively charged 1-palmitoyl-2-oleoyl-phospatidylserine (POPS) and D31-POPS from Avanti Polar Lipids (Alabaster, Alabama, US). The lipids were dissolved in chloroform/methanol (Sigma-Aldrich) 2:1, mixed in the desired ratio and gently dried under a nitrogen flux. Solvent traces were removed under vacuum, overnight. The lipid mixtures were then resuspended in Milli-Q water (Millipore, resistivity 18.2 MΩ cm), in a concentration of 0.5 mg/ml, vortexed and let to swell for 30 min. The resulting opalescent suspension was extruded at least 19 times through polycarbonate membranes with pores of 50 nm using a commercial extruder (Avestin, Mannheim, Germany). The obtained unilamellar vesicles (ULV) were then diluted 5 fold and administered to the solid support in the liquid cell either for NR or for AFM-FS. The incubation time to allow vesicle fusion and lipid bilayer formation varied between 20 and 60 min. The cell was gently rinsed with Milli-Q water to remove the vesicle in excess. The lipid composition was either pure POPC, or POPC/POPS 9:1 mol/mol.

2.2. Beta-amyloid

Aβ(1–42), purchased from Bachem (Germany) was pretreated with trifluoro acetic acid (TFA, Sigma Aldrich) in concentration 0.5 mg/ml [30] to destroy seeds and aggregates. The desired amount was then dried under a nitrogen stream and re-dissolved in H_2O (for AFM) or D_2O (for NR) with concentration 0.1 mg/ml. The peptide was administered to the cell containing the supported membrane at a 1 μM concentration and let to incubate 30 min before changing the liquid subphase to remove the peptide in excess.

2.3. Polyelectrolytes

To prepare the polymer cushion we used poly(ethyleneimine) (PEI, M_w ~ 55,000) and poly(allylamine hydrochloride) (PAH, M_w ~ 70,000) as polycations and poly(styrene sulfonate sodium salt) (PSS, M_w ~ 70,000) as polyanion. The polyelectrolytes were purchased from Aldrich Chemical Co and used without any further purification. Polyelectrolytes were solved in aqueous solution of 1 M NaCl in a monomer concentration of 10^{-2} M except for PEI, which was dissolved in pure H_2O.

2.4. Preparation of PEM

For solid supported samples, freshly cleaved muscovite mica (Agar Scientific, U.K.) was used; for polymer supported membranes, the substrate was silicon or glass. Glass coverslips or silicon substrates (24×24 mm^2) were cleaned by heating to 75 °C for 10 min in a mixture of H_2O:H_2O_2:NH_4OH 5:1:1 v/v/v to remove organic impurities (RCA cleaning method).

H_2O_2 (p.a. 30% aqueous solution) was purchased from Fluka; NH_4OH (p.a. 28% aqueous solution) was a product of Sigma.

Polyelectrolyte multilayers (PEM) were deposited layer-by-layer according to the procedure introduced by Decher [16]. After the cleaning procedure the substrates were negatively charged. They were embedded for 20 min in the PEI cationic solution for the deposition of the first layer, and subsequently in PSS and PAH solution

recursively, again for 20 min. Each polyelectrolyte deposition was followed by triple rinsing in Milli-Q water for 2 min. PEM was always terminated with the cationic PAH as outermost layer. We deposited PEM according to the sequence PEI(PSS/PAH)$_5$, unless otherwise specified in the text. In the neutron reflectivity experiments the last PSS/PAH layers were freshly prepared *in situ* in the sample chamber of the reflectometer, just before vesicle injection.

2.5. Neutron reflectivity

NR measurements were performed at the V6 reflectometer at the BER II research reactor of the Helmholtz-Zentrum Berlin. The neutron wavelength was 0.47 nm and the experiment was performed in θ/2θ geometry consuming about 7 h beamtime per complete run. The rectangular beam was set by a slit system in front of the sample. The polymer cushion was deposited onto silicon blocks 10 cm × 5 cm × 1.5 cm in size, previously treated according to the procedure already described. The flow cell used for the experiments consists of a Teflon trough with a depth of 3 mm, sealed with an O-ring to the silicon block. The liquid content of the chamber is 15 ml. The chamber had an inlet and an outlet through which it was possible to exchange the liquid subphase. The construction details are reported in Howse al. [31]. The supported lipid membrane was formed injecting 15 ml of vesicle suspension either in PBS buffer or in D_2O into the chamber. The phospholipids used in these experiments were partially deuterated, i.e., D31-POPC and D31-POPS, to index-match the PEM and to obtain a higher contrast for the hydrogenated Aβ(1–42). After an incubation time of 20 min the subphase was exchanged to buffer (or D_2O) in order to eliminate the vesicle excess. The same procedure was followed to inject the peptide in the chamber, when studying the effect of Aβ on the supported membrane.

The liquid subphases were always degassed before use.

In the configuration used, the aqueous medium, i.e. D_2O, had an SLD higher than the solid lid, i.e. the silicon block. Therefore, total reflection occurred below a critical Q_c value. Beyond Q_c, the reflectivity R decays with Q^{-4} and the shape of the reflectivity curve is a function of the averaged SLD profile in direction normal to the interface. The information extracted from a single NR measurement are the layer thickness d(Å), the scattering length density ρ(z) along the normal to the interface, and the roughness σ between the interfacial layers.

2.6. AFM imaging and Force Spectroscopy

All AFM measurements were performed by using a Nanowizard II (JPK Instruments, Germany) mounted on an Axio Observer D1 (Carl Zeiss, Germany) inverted optical microscope. V-shaped gold-coated silicon nitride cantilevers (NPS, Veeco Instruments, USA), with a nominal spring constant of 0.06 N/m and of 0.32 N/m respectively and pyramidal tip with typical curvature radius of 10 nm were used. All substrates (i.e., mica, silicon or glass coverslips) were fixed in a Petri dish by using a two-component epoxy glue and the AFM measurements performed inside the Petri dish itself. The samples were always kept in aqueous subphase. AFM images were collected using tapping mode, working in liquid environment.

Force spectroscopy maps were acquired in contact mode. In force mapping, a sequence of force distance curves was collected over at least 5 different areas of the supported membrane. The areas had a dimension of 1 μm × 1 μm and were divided in grids of 25 × 25 sampling points. In each point an extension–retraction force–distance curve was recorded. The applied load was in the range of 8–15 nN, the curves length was 350 nm and the tip velocity of 700 nm/s was maintained constant.

For each sample at least 5 maps consisting of 625 force–distance curves were collected and analyzed using a home built algorithm.

2.7. Light scattering

Dynamic light scattering (DLS) measurements were performed with a Malvern Zetasizer instrument at a protein concentration of 0.025 mg/ml and 0.1 mg/ml. Aβ(1–42) was dissolved in PBS pH = 7.4, after pretreatment in TFA and centrifugation for seed removal, as described previously [5]. The measurements were taken right after centrifugation, 1 and 4 days after, respectively.

3. Results

3.1. Neutron reflectivity

3.1.1. Refining the protocol for membrane formation

Neutron reflectivity was essential in refining the protocol for the preparation of a bilayer by vesicle fusion on the surface of a polyelectrolyte multilayer (PEM).

As mentioned in Section 1, the process of vesicle fusion and lipid bilayer formation at the charged polymer surface is a complex phenomenon and depends on several factors. We found that not only the vesicle and interface compositions play a role in it, but also the aging of the surface and the presence of salts in the subphase are critical parameters to be controlled to obtain reproducible results.

All NR experiments were performed in a special flow cell available at the V6 beamline at the BER II research reactor of the Helmholtz-Zentrum Berlin. The cell consists of a thick silicon block, transparent for the neutron beam, on top of which the polymer cushion is deposited according to the procedure described in the literature [32] and reported in Section 2. A cartoon of the cell and of the experiment is reported in Fig. 1; detailed information on the cell is available elsewhere [31,33]. The silicon block acts as the lid of a Teflon cell containing the liquid subphase in which the vesicles are injected to

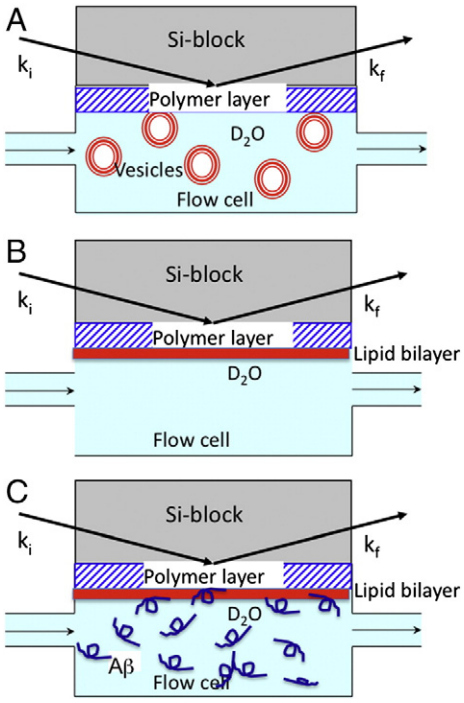

Fig. 1. Sketch of the liquid cell in use at the reflectometer V6: a thick silicon block precoated with a polyelectrolyte cushion acts as lid of a water filled Teflon reservoir and is covered with the polyelectrolyte cushion at the water side; the neutron beam impinges on the solid–liquid interface through the silicon backing (A). In the experimental sequence, first the vesicles are injected in the subphase to allow for bilayer formation at the surface of the polymer cushion against the liquid phase. The subphase is subsequently displaced by pure D_2O for removing excess lipids (B); then, the peptide is injected into the cell to study its effect on the supported lipid membrane (C).

form the lipid bilayer. The subphase can be exchanged according to the experimental needs. By using this cell it is therefore possible to study a supported lipid membrane in aqueous buffer, and to monitor *in situ* the changes induced by the exchange of the buffer or by injecting in it a chemical agent, the peptide Aβ(1–42) in our case.

To obtain reproducible formation of a membrane, it was necessary that the outermost anionic–cationic PEM bilayer of the polymer cushion was freshly deposited *in situ* in the flow cell at the V6 reflectometer at the beginning of the experiment. A lipid mixture resembling the phospholipid composition of a neural membrane in terms of acyl chain unsaturation and head group charge was chosen, i.e., D31-POPC/D31-POPS 9:1 mol/mol. The phospholipids used in these experiments were partially deuterated to index-match the PEM and obtain a higher contrast for the hydrogenated Aβ(1–42). Fig. 2 shows (black triangles) the reflectivity curve of PEI/$(PSS/PAH)_5$, the typical polyelectrolyte cushion used in the experiments. The subphase was PBS buffer in D_2O or pure D_2O when specified, to improve the contrast to the partly hydrogenous lipid membrane and to reduce the background scattering due to the incoherent scattering of hydrogen. The periodicity of the interference or so-called Kiessig fringes corresponds to a thickness of the PEM cushion of about 300 Å (see Table 1) as expected from literature [34]. In a first attempt we injected D31-POPC/D31-POPS vesicles in PBS in a subphase in the flow cell with the same PBS buffer (13.7 mM NaCl). No formation of supported lipid bilayers could be achieved. The same negative result was observed with zwitterionic D31-POPC vesicles in pure D_2O (data not shown). On the contrary, when injecting D31-POPC/D31-POPS vesicle dispersion in the cell containing D_2O, a bilayer formation was observed within 20 min. Fig. 3 reports the kinetics of bilayer formation. The intensity of the first minimum at $Q = 0.028\ Å^{-1}$ in the reflectivity curve of PEM was monitored versus time after injection of vesicles in the cell; an increase of the counting rate indicates a shift of the minimum and therefore a change in thickness of the interface. As shown in Fig. 3, within 20 min the counting rate was stabilized, indicating that the system reached an equilibrium configuration. The reflectivity curve measured after an incubation time of 2 h is reported in Fig. 2. Once the bilayer was formed, it was possible to exchange the subphase in the flow cell from D_2O to PBS, with a detectable effect on the reflectivity curve, as shown in the same figure.

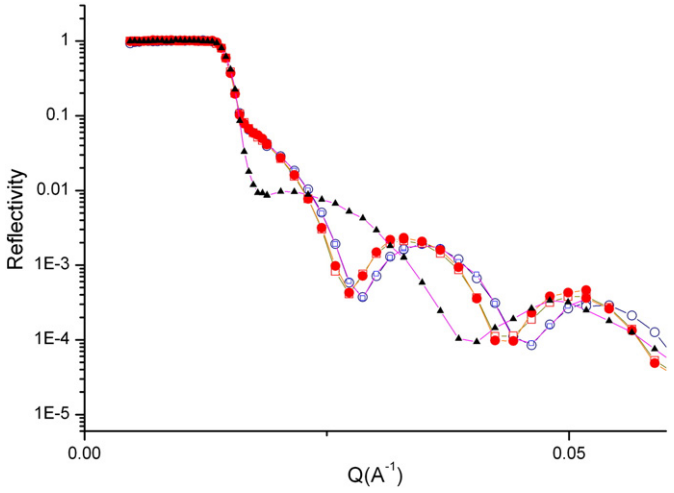

Fig. 2. Reflectivity curves from PEM in D_2O (black triangles) and subsequent D31-POPC/D31-POPS vesicles adsorption (blue open circles), as revealed by the reduced distance ΔQ of adjacent minima positions and shift of the Kiessig fringes to lower Q; the exchange of the subphase to PBS first (red open squares) and then to D_2O (blue open squares) causes a reversible swelling of the structure. The reversibility is demonstrated by a further exchange from D_2O to PBS buffer (red filled circles).

Table 1
Structure of lipid bilayer membranes on polyelectrolyte cushions as extracted from the best fits to the experimental data.

		Thickness t (Å)	10^6·SLD ($Å^{-2}$)	Roughness σ (Å)
D_2O				
1	PEM	292	4.02	14.3
2	Lipid membrane	54	3.84	5.0
3	Subphase		6.26	2.0
1	PEM	292	4.02	14.3
2	Lipid membrane with Aβ(1–42)	57	3.74	5.0
3	Subphase		6.26	2.0
PBS				
1	PEM[a]	321	3.97	16
2	Lipid membrane	48	3.90	5.0
3	Subphase		6.29	
1	PEM	304	3.92	10
2	Lipid membrane with Aβ(1–42)	52	3.59	9.4
3	Subphase		6.19	2.0

[a] This measurement was performed on a different beamtime, with a PEM consisting of 6 instead of 5 (PSS/PAH) double layer pairs.

The data were fitted with a simple slab model with a layer corresponding to the PEM cushion and a layer corresponding to the lipid bilayer. Table 1 contains the parameters of the fit, i.e., layer thickness *d*, scattering length density SLD (*z*) of the layers and roughness σ, as obtained in the two different subphases. Due to beamtime constraints it was not possible to perform a contrast variation and measure more independent reflectivity curves. The thickness of the PEM cushion was between 293 Å and 304 Å depending on the buffer condition, as expected for this polyelectrolyte combination. The fitted scattering length density ranged from $3.92 \cdot 10^{-6}\ Å^{-2}$ to $4.02 \cdot 10^{-6}\ Å^{-2}$, in accordance with the value calculated from the molecular structure of the compounds and the respective water content, as also found in similar systems [34]. The thickness of the D31-POPC/D31-POPS membrane as determined from the fit was 54 Å in D_2O and 48 Å in PBS, in perfect agreement with the literature [7].

The surface coverage of the lipid bilayer calculated by taking into account the D_2O content of the lipid layer was about 75%.

3.1.2. Penetration of Aβ(1–42) in the lipid membrane

When a stable lipid membrane was formed on the polymer cushion, the administration of Aβ(1–42) into the subphase caused a change in the reflectivity curve and in the profile of the membrane. We were interested in the study of soluble species of Aβ(1–42); therefore Aβ(1–42) was pretreated prior to the experiment as described in Section 2 and it was always freshly prepared. The

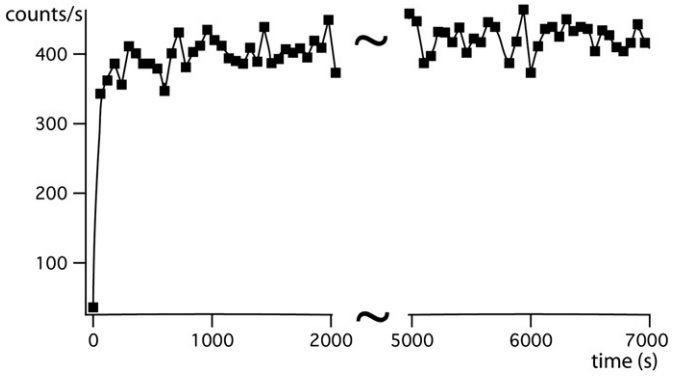

Fig. 3. Kinetics of bilayer formation on top of the PEM. The counting rate at the first minimum of the reflectivity curve at $Q = 0.028\ Å^{-1}$ increases over minutes and stabilizes after circa 2000 s. The time interval between 2000 s and 5000 s has been removed from the graph.

absence of large aggregates of Aβ(1–42) in the liquid subphase was proven by dynamic light scattering (DLS) measurements. The results obtained from peptide solutions at two different concentrations, i.e. 0.03 mg/ml and 0.1 mg/ml, are listed in Table 2. The lower concentration is the same used in all the other experiments. In this condition, the average size of the particles in solution (R_H) is 1.2 nm right after preparation (t = 0.5 h), indicating the presence of monomeric species. Repetitions of DLS measurements of the same Aβ(1–42) solution over time showed the presence of aggregates with an average size larger than 160 nm after 4 days, i.e., after a much longer time than the acquisition time typical for a NR measurement. A dependence of aggregate size upon peptide concentration was observed.

Fig. 4A and B shows the reflectivity curves before and after interaction of Aβ(1–42) in D_2O and PBS buffer solution, respectively. The curves obtained from PEM cushion (black, diamonds), from the lipid membrane (red, circles) and from the membrane in presence of peptide (blue, squares) are displayed along with the best fits (solid lines). A small but clear shift of the reflectivity curves measured after interaction with the peptide is visible in both cases. Fig. 5A and B contains the interface profiles used to obtain the best fit of the reflectivity curves (solid lines in Fig. 4). The fit parameters are listed in Table 1.

In the presence of Aβ(1–42) the thickness of the bilayer increases from 54 Å to 58 Å in D_2O and from 48 Å to 52 Å in PBS buffer solution.

In the presence of Aβ(1–42) the membrane profile in the z direction, perpendicular to the membrane plane, is heavily affected. A lowering of the average scattering length density is obtained, and it is especially visible in PBS buffer: upon interaction with Aβ(1–42) the inner structure of the lipid membrane is heavily perturbed and this effect is enhanced in physiological conditions.

Besides the already described major finding, the experiments conducted by NR had two additional outcomes. After measuring the scattering curve in the presence of Aβ(1–42), we injected again D31-POPC/D31-POPC vesicles in the flow chamber, to check if a second bilayer could be built on the top of the first one. In fact, we had previously observed that Aβ(1–42) has a fusogenic activity to unilamellar vesicles [5]. In our previous study the vesicle radius reached a stable maximum at 33 nm and beyond this no vesicle fusion took place. In the current investigation this effect was not observed. The result that Aβ could not fuse additional vesicles to the planar lipid bilayer strengthens the notion that the curvature of the membrane plays an important role in this scenario.

Furthermore, we succeeded in removing the lipid membrane on top of the PEM by injecting ethanol in the flow chamber, incubating it for few minutes and rinsing three times with D_2O after several minutes. This finding adds no information to our study on Aβ; we report it though, since the possibility to remove the membrane *in situ* can be exploited to accelerate the experimental procedure and overcome beam time constraints typical of NR experiments.

3.2. AFM

To gain supplemental information about the changes caused on the lipid membrane by interaction with Aβ(1–42), we investigated samples homologous to those investigated by NR by advanced AFM technique. The model system is the same besides the substrate (glass or mica instead of silicon) and the size of the samples, much smaller for this second investigation. AFM can achieve a local mechanical characterization of small areas of the samples. To arrange the sample on the AFM, the cell is open and the substrate holding the membrane is sitting at the bottom, with the sample facing the liquid phase. The polyelectrolyte multilayers were freshly deposited on mica or on glass cover slips. According to the knowledge acquired by the NR experiments on the kinetics of formation of the lipid bilayer, the ULV were introduced in the liquid cell containing the substrate decorated with the PEM and let to incubate for 20–30 min at room temperature to allow vesicle fusion and bilayer formation. Since for the AFM experiment we were not restricted to limited beam time as in the NR experiments, we also compared the behavior of lipid bilayers supported on mica and polymer cushion, to investigate the influence of the substrate.

Table 2
R_H from dynamic light scattering measurements of Aβ(1–42) in aqueous solution as a function of time and of peptide concentration.

Time	Aβ concentration	Aβ concentration
	0.03 mg/ml	0.1 mg/ml
	R_H	R_H
0.5 h	1.3 ± 0.2 nm	23 ± 5 nm
12 h	6.3 ± 0.3 nm	36 ± 12 nm
72 h	161 ± 43 nm	230 ± 101 nm

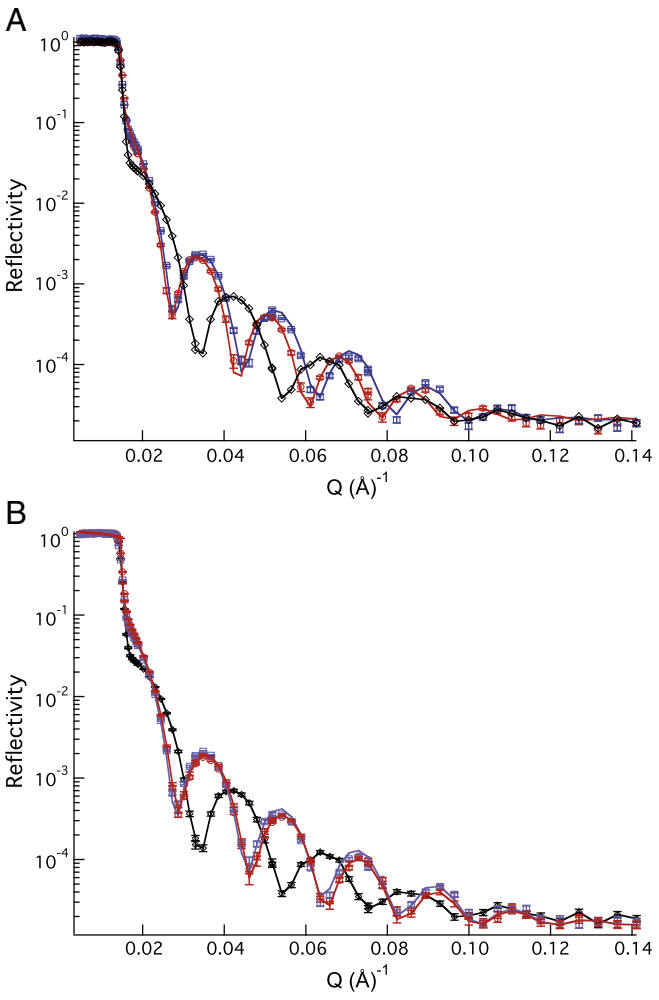

Fig. 4. A: Reflectivity curve of PEM (black, diamonds), of PEM with adsorbed lipid membrane before (red circles) and after (blue squares) interaction with Aβ(1–42), in D_2O. B: Reflectivity curve of PEM (black diamonds), of PEM with adsorbed lipid membrane before (red circles) and after (blue squares) interaction with Aβ(1–42), in PBS.

3.2.1. Topography of lipid bilayers

Topographical images of the lipid bilayers are displayed in Fig. 6. The top panels show a POPC/POPS membrane on mica (Fig. 6A) and on PEM (Fig. 6B). The lipid bilayer on mica, as expected, covers the substrates homogeneously, apart from a few regions. The topography

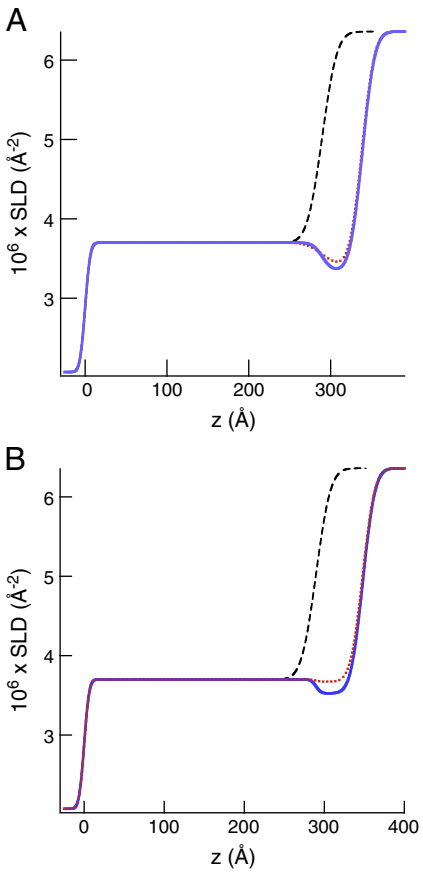

Fig. 5. Models of the scattering length density profiles used to fit the experimental reflectivity curves of the membranes on polymer cushion in the case of D_2O (A) and PBS buffer (B). (PEM (black, dashed), PEM with lipid membrane before (red, dotted) and after (blue, solid) Aβ(1–42) injection).

of the PEM supported membrane is less defined, because of its floating character, because of the increased roughness of the underlying PEM and because of the potentially increased softness of the supported membrane [35]. The AFM phase signal (Supplemental Material) shows a clear difference of the PEM surface before and after bilayer formation, confirming that the vesicle fusion successfully happened.

The bottom panels show the same areas after interaction with freshly prepared Aβ(1–42). Small annular structures, indicated by the arrows, are visible in the mica supported lipid bilayer (Fig. 6C). Additionally, bigger aggregates (height ~ 20 nm) appear to be randomly adsorbed to the surface.

The topography of the PEM supported lipid bilayers appears to be affected by Aβ(1–42) but the peptide is difficult to visualize due to the intrinsic disorder of the surface. Some information is nevertheless extracted from the phase TM-AFM and reported in the Supplemental Material.

3.2.2. Mechanical stability of the lipid bilayers by AFM-FS

Force spectroscopy measurement were performed typically on areas 1 μm × 1 μm with a 40 nm resolution in x and y direction.

As already reported in the literature, a discontinuity point, which denotes a breakthrough event, i.e., the penetration of the tip through the membrane, characterizes a force–distance curve for a solid supported lipid bilayer. Fig. 7 displays the force distance curves obtained by approaching the AFM tip to a POPC/POPS double layer on mica (Fig. 7B) and on PEM (Fig. 7C). The same figure shows the force distance curve obtained approaching the tip to a bare PEM interface (Fig. 7A) which was PAH terminated: the attractive force between substrate and tip is followed by a very steep force increase. The AFM tip is negatively charged at this pH and is therefore attracted by the positively charged groups of PAH.

In the case of membranes supported on mica (Fig. 7B), the breakthrough point is single and the statistical distribution of the yield forces is Gaussian, as expected, and centered at a central value of 3.5 nN (Fig. 8A).

In the case of PEM supported membranes, as thoroughly discussed in our previous paper [29], force–distance curves have different behavior (Fig. 7C): they exhibit a long range effect in the contact region; in some cases, they present a second discontinuity point; and, more important to our findings, the statistical distribution of the breakthrough forces has a bimodal character (Fig. 8B). To avoid confusion, the bimodal character is not related to the presence of the second discontinuity in the curve, but it holds true for the single event curves, which are the majority fraction. As shown in Fig. 8B, the centers of the two Gaussian distributions correspond to forces of 2.3 nN and 6.0 nN, respectively.

Upon addition of Aβ(1–42) in the liquid subphase on top of the bilayers, at a concentration 1 μM, the following results were obtained. In the case of mica supported POPC/POPS bilayer, the breakthrough event occurs at a much lower force (1.2 nN) and the force distribution maintains a single Gaussian profile (Fig. 8A, empty bars). Remarkably, the same effect is obtained also with a very diluted concentration (5 nM) of Aβ(1–42) (data not shown). In the case of PEM supported lipid membranes, after interaction with Aβ(1–42) the distribution of the breakthrough peaks looses its bimodal character and the rupture events are all distributed around a value of 2.3 nN (Fig. 8B). The force–distance curves do not contain double breakthrough peaks.

Additional information coming from the AFM investigation is the quantification of the substrate coverage by the lipid bilayer. In the surface mapping indeed 85% of the force distance curves show a successful penetration event of the tip for sample supported on mica; the percentage is lowered to 67% in the case of PEM supported membranes. This percentage represents the lower limit of the lipid covered area, if we presume that it is statistically possible that the breakthrough does not occur even in areas covered by the membrane.

4. Discussion

Within this work we have addressed two different issues. The first was the control of the conditions necessary to obtain a single membrane of POPC/POPS on top of a polyelectrolyte cushion. The second issue was the interaction of the polymer supported lipid bilayer with the Alzheimer's peptide Aβ(1–42). Two different techniques have been applied, namely neutron reflectometry and AFM Force Spectroscopy. These two techniques allow to study at physiological conditions a supported lipid membrane kept in its fluid state, in aqueous environment and they offer the possibility to correlate structural information to local mechanical properties of the membrane. To the best of our knowledge, NR and AFM-FS have been combined for this purpose for the first time. It seems important to highlight that in both experimental set-ups a single lipid bilayer is studied in aqueous environment and that it is possible to change the experimental conditions like pH or ionic strength *in situ* and to monitor on line the variation induced in the system.

4.1. Vesicle fusion and lipid bilayer formation

Vesicle adhesion and fusion need a high affinity between lipids and support, whereas the formation of a continuous lipid layer requires the mobility of lipids at the interface. The success of bilayer formation depends on the properties of the interface and of the lipid mixture, as well as on other parameters like concentration, temperature, pH and ionic strength of the solution [17,18]. Up to date, a systematic knowledge of this process is still missing.

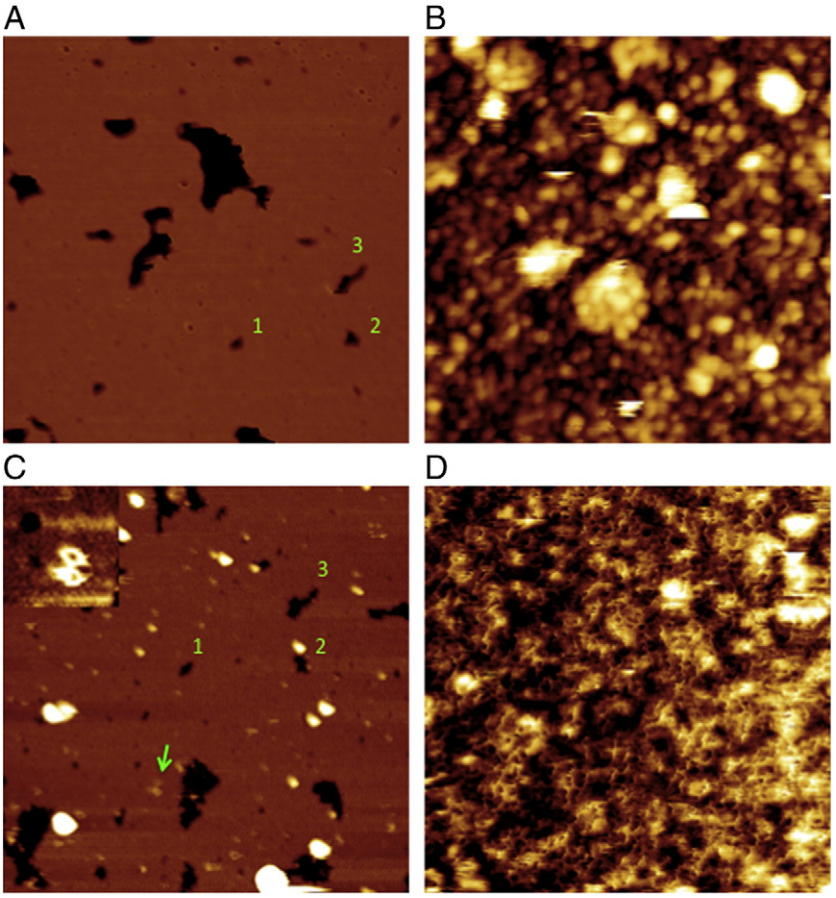

Fig. 6. Topography of POPC/POPS bilayers adsorbed on mica (left panels A, C) and on polymer cushion (right panels B, D). A and B show the lipid bilayers before exposure to Aβ(1–42), C and D after Aβ(1–42) injection. In C, small doughnut-shaped Aβ aggregates (indicated by the arrow and enlarged in the inset) appear in the membrane; bigger aggregates (lateral dimension up to 70 nm, thickness 2–10 nm) are randomly adsorbed to the membrane surface. The area imaged after exposure to Aβ (6 C) is slightly shifted with respect to A, as recognizable by the gaps in the bilayer, indicated with 1, 2 and 3. The topography of the lipid bilayer on PEM is affected by the presence of Aβ(1–42) (D) but the localization of the peptide is not straightforward. The images obtained from bilayers on PEM are much fuzzier because of the softness of the sample. Data scale (A, B, C, D): 1 μm; z-range = 4.8 nm (A), 14.3 nm (B) 4.8 nm (C), 14.3 nm (D); inset: 140 nm, z-range 0.7 nm.

By NR it was established here that, in order to achieve reproducible results, the polyelectrolyte cushion must be freshly prepared, just before vesicle spreading. Aging of the surface might lead to decrease of the surface charge of the polyelectrolyte surface or other alterations and prevent successful vesicle adhesion (see Table 2).

As expected, we observed that the thickness of the polymer interface is modulated by the buffer concentration, which controls the swelling of the polyelectrolyte film [34,36]. In our case, we found the thickness of the polymer cushion, i.e., PEI/$(PSS/PAH)_5$ to vary from 293 Å in pure D_2O to 304 Å in PBS (13.7 mM NaCl).

Our results show that in pure D_2O, a positively charged interface is suitable for fusion of vesicle composed of an anionic lipid mixture (POPC/POPS 9:1 mol/mol), but not for fusion of a zwitterionic vesicle (POPC). The process is clearly dominated by electrostatic forces. In addition, the same anionic lipid mixture did not attach to the interface when the surface charge was screened by the presence of salt (PBS, 13.7 mM NaCl). This finding is in agreement with the study of Fischlechner [37] in which spreading of vesicles on PEM was investigated by several techniques and found to be dependent on the vesicle composition.

After formation of the bilayer it is possible to exchange the liquid subphase from D_2O to PBS buffer: the membrane remains attached to the polymer and a swelling effect is recorded, reversible and reproducible. This fact allows performing experiments in physiological conditions. The successful route for bilayer formation (Table 3) was therefore applied to all of subsequent experiments either by NR or by AFM. The successful preparation of a continuous lipid membrane is demonstrated by the reflectivity curve, resulting from a continuous interface extending on the whole substrate area and is directly supported by the AFM imaging. The surface coverage as determined by NR is about 75%, a value similar to that obtained by NR in the case of lipid membranes formed by Langmuir deposition on bare silicon [38].

The kinetics of bilayer formation is fast compared to the recording time of a NR curve: after few minutes a homogeneous lipid interface is built and it remains stable for days.

The structural parameters extracted by NR are in perfect agreement with the literature. A membrane thickness of 54 Å is indeed typical of a POPC/POPS bilayer as we had already measured by neutron diffraction on multilayers at 98% r.h. The thickness change upon buffer exchange is little (about 2 Å). The AFM image of the membrane supported on PEM is not as smooth as the one obtained on mica. This is probably due to the high lateral mobility of the bilayer and to the increased roughness of the PEM cushion.

4.2. Interaction of neurotoxic Aβ(1–42) with polymer supported bilayers

It is well known that Aβ species at different aggregation stages interacts differently with the cellular membranes. In our study we considered only freshly prepared Aβ samples, in the attempt to maximize the presence of small, membrane soluble peptides. DLS measurements have shown, in solution, the absence of aggregated species (Table 2) at the beginning of each experimental trial. The kinetics of aggregation has been shown to be concentration dependent.

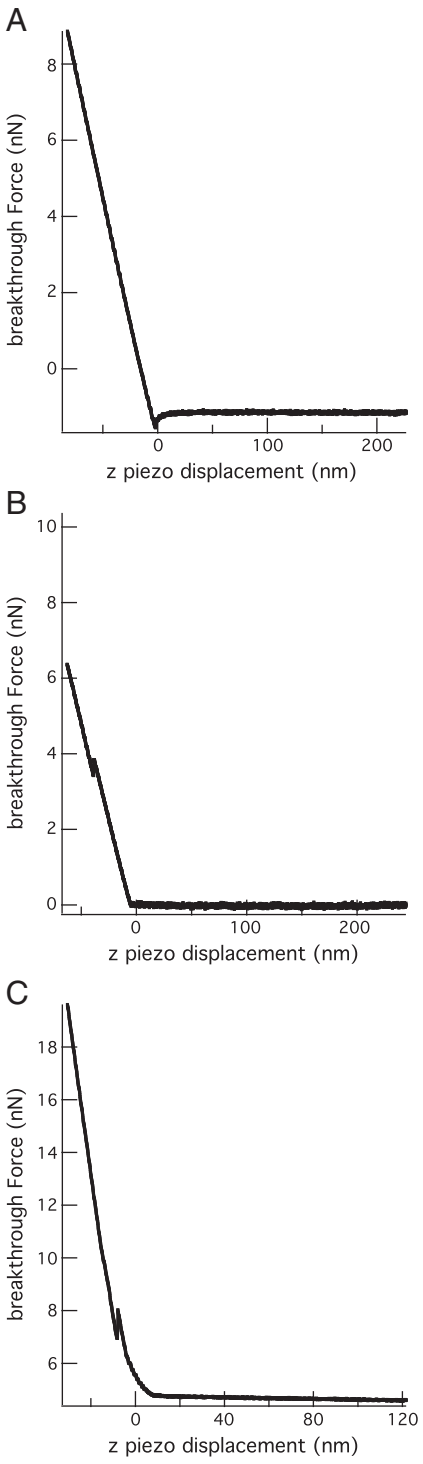

Fig. 7. Force–distance curves obtained from of polymer cushion (A), mica supported lipid membrane (B) and of PEM supported lipid membrane (C). In the case of PEM alone the attractive force between tip and surface generates the dip at $z = 0$ before the steep slope of the curve for $z < 0$ nm. The discontinuity in the curve obtained from lipid bilayers (B and C) is the breakthrough. For polymer supported membranes (C) a long-range effect is observed in the contact zone between tip and surface.

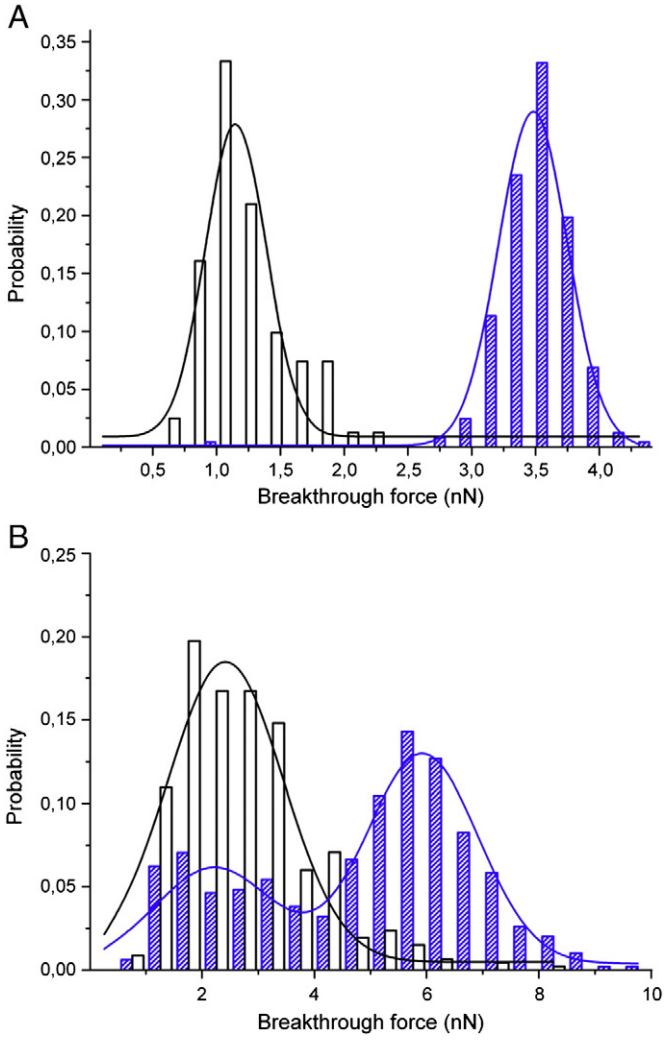

Fig. 8. Histograms of the breakthrough forces measured on mica (A) and on polymer cushion (B). A: The force distribution of membranes on mica is unimodal (full bars) and can be described with a single Gaussian function (solid line). After interaction with Aβ(1–42) the distribution on mica shifted towards lower forces (empty bars). B: On PEM, the force distribution for membranes is bimodal and can be described by two distinct Gaussian functions (full bars). The bimodal character of the distribution is lost after Aβ(1–42) incubation and the mean value of the breakthrough forces is about 2.3 nN (empty bars).

AFM images revealed the presence of small structures, in the nanometer size, in the POPC/POPS lipid bilayer supported on mica. Some of these structures appear to be annular, supporting the hypothesis of barrel like, pore forming Aβ species [39,40]. Moreover, globular bigger aggregates are randomly adsorbed to the membrane surface. These aggregates have not been detected in solution by DLS at the same aggregation time: hence, the kinetics of aggregation is affected by the interaction with the lipid membrane [41].

The effect of Aβ species on solid supported bilayers was explored in recent years by several techniques, especially by AFM. These studies showed that bilayers of DMPC and of total lipid brain extract were partially destroyed after interaction with Aβ(1–40) [25]; more recently it was shown that Aβ interacts preferentially with solid domains of a lipid bilayer [42]. Tethered membranes were used as a model to study the interaction of soluble Aβ(1–42) protofibrils by NR [43].

In our study we have extended the investigation to membranes on polymer cushion, which have different behavior from solid supported

Table 3
Conditions of bilayer formation at 25 °C.

PEM (+)	Lipid vesicles			Ionic strength	
Fresh	1	Zwitterionic	0	Pure D_2O	1
Aged	0	Charged (−)	1	PBS buffer	0

Successful route: PEM (fresh) × Lipid vesicles (charged) × Ionic strength (pure D_2O) = 1.

ones and resemble more closely the neural membrane in its natural environment.

As shown by the reflectivity curves, there is interaction between the lipid double layer and the Aβ(1–42); the membrane profile is modified in the presence of Aβ(1–42): the mean value of the scattering length density of the membrane is lowered by about 10% in D_2O (see Table 1) meaning that a non-deuterated molecule is penetrating the membrane. The thickness of the lipid bilayer increases in the presence of Aβ(1–42) by about 4 Å. This concomitant effects reveal that Aβ(1–42) is capable of penetrating the double layer, increasing the thickness of the membrane and changing its scattering profile. In our previous investigation on lipid vesicles by small-angle neutron scattering, we had observed a thinning of the vesicle shell (i.e., the lipid bilayer) upon interaction with Aβ(1–42); the effect was dependent on the pH. The differences between the two investigated systems and between the two techniques explain this contradiction. First of all, the system investigated by NR is a planar bilayer on stratified polymer support, whereas in the SANS experiment the curved bilayer experiences an aqueous environment on both sides. Moreover, by SANS the main contribution to the scattering signal comes from the deuterated hydrocarbon chains of the lipids; in the NR experiment the thickness of the interface obtained from the fit, includes also the water shell between support (PEM) and membrane. An increase of hydration of the polar heads (which indeed was observed by SANS) results then in an increase of the interface thickness measured by NR. The thickness change of the bilayer in the presence of the peptide was not observed in our previous study by neutron diffraction from stacked lipid on solid support; this is a clear indication that a membrane supported on polymer cushion and studied in aqueous buffer is better suitable to study the interaction between proteins and membranes.

Unfortunately, the NR experimental resolution does not allow determining the location of Aβ in the lipid double layer. From our reflectivity data the possibility of Aβ adsorption on top of the membrane could not be ruled out. We have other experimental evidence, i.e., data obtained by neutron diffraction on stacked bilayers, that show a perturbation of the membrane profile by Aβ(1–42) in the region of the hydrophobic core (unpublished results); these data support therefore the interpretation of Aβ insertion versus adsorption. Moreover, the interpretation is corroborated by our previous findings obtained by neutron diffraction on lipid multilayers: in that case the short analogue Aβ(25–35) was unequivocally localized in the hydrophobic core of the bilayer [7].

As mentioned above from the NR measurements alone the local placement of Aβ within the lipid membrane cannot be resolved. In principle Aβ can insert into the membrane and/or show preferential adsorption to the edges (defect sites) of the PEM-supported lipid bilayers. From a simplified calculation, however, we can achieve an estimate of the total amount of Aβ inserting in and adsorbing to the membrane:

Before incubation with Aβ we have

$$SLD_{Lipid\_membrane} = \Phi_{Lip} SLD_{Lip} + \left(1-\Phi_{Lip}\right) SLD_{water} \quad (1)$$

After incubation with Aβ we have:

$$SLD_{Lipid\_membrane+A\beta} = \Phi'_{Lip} SLD_{Lip} + \Phi_{A\beta} SLD_{A\beta} + \left(1-\Phi'_{Lip}-\Phi_{A\beta}\right) SLD_{water} \quad (2)$$

Hence

$$\Phi_{A\beta} = \frac{SLD_{Lipid\_membrane\ +\ A\beta} - SLD_{water} - \Phi_{Lip'}\left(SLD_{Lip} - SLD_{water}\right)}{SLD_{A\beta} - SLD_{water}} \quad (3)$$

with $\phi_{Lip}' = \phi_{Lip}$, i.e., constant amount of lipids within the bilayer membrane, $SLD_{Lip} = 2.81 \cdot 10^{-6}\,Å^{-2}$ ($SLD_{D31\text{-}POPC}$), $SLD_{A\beta} = 2.97 \cdot 10^{-6}\,Å^{-2}$ ($SLD_{protein}$ in D_2O) after [44], with $SLD_{Lipid\_membrane}$, SLD_{water} and $SLD_{Lipid\_membrane+A\beta}$ taken from their respective values as gathered in Table 1, we estimate $\phi_{A\beta}$ in the bilayer membrane against D_2O to be 0.07 and against PBS buffer to be 0.15. On average we thus have $\overline{\Phi}_{A\beta} = 0.11 \pm 0.06$.

The maximum total amount of Aβ in multilayer membranes is reported to be 3% mol or $X_{A\beta} = 0.03$ [7]. That number corresponds to a volume fraction of Aβ of

$$\Phi_{A\beta} = \frac{x_{A\beta} V_{A\beta}}{x_{Lip} V_{Lip} + x_{A\beta} V_{A\beta}}$$

with $V_{A\beta}$ taken to be equal to 5470 $Å^3$[45] and $V_{lip} = 1267\ Å^3$[46], $\phi_{A\beta,max}$ is 0.12 in close match with our results on the single polymer supported lipid bilayers presented in the current study.

AFM-FS has shown that the mechanical properties of the membrane are different depending on the substrate. On mica the force necessary to punch through the double layer is lowered in presence of Aβ, meaning that the structural changes upon interaction with the AD peptide have a softening effect on the bilayer. The force necessary to penetrate the double layer decreases noteworthy after interaction with Aβ(1–42); this effect is substrate dependent. On PEM the force distribution is bimodal: there are regions more and less tightly packed. This can be due to local discontinuities and fluctuations on the charge distribution of the polyelectrolyte surface. After interaction with the peptide, the bimodality of the force distribution disappears; apparently, the peptide interacts more strongly with the more packed regions of the membrane supporting a preferential insertion of Aβ(1–42), as also seen in the gel phase of DPPC bilayers [42].

The lowered mechanical stability of the lipid membrane found by AFM-FS is in agreement with the decreased water content of the membrane seen by NR. This finding is important in the AD scenario, since it means that soluble species of Aβ(1–42) interacts deeply with the neural membrane, changing its structure but especially softening the neural membrane.

5. Conclusions

In this paper two different techniques have been concomitantly employed to study structural and mechanical properties of lipid membranes supported on polymer cushion, i.e., neutron reflectivity and AFM Force Spectroscopy. A reproducible protocol for the preparation of a supported phospholipid membrane with composition mimicking the neural membrane and under physiological condition (PBS buffer, pH = 7.4) was refined. In particular the change in structure and local mechanical properties of the lipid membrane in the presence of medically relevant peptides like Aβ(1–42) have been investigated. Aβ(1–42) was found to interact strongly with the supported membrane, inducing both a structural change (i.e., it penetrates into the membrane), and inducing a softening of the lipid bilayer. Penetration into the bilayer is also supported by AFM imaging: Aβ(1–42) annular structures in the nanometer size have been detected in POPC/POPS lipid membranes on mica, supporting the hypothesis of pore forming Aβ species. We may postulate that the observed mechanical softening of the membrane is due to the increased lateral diffusion of the membrane lipids after interacting with Aβ as recently observed by quasi-elastic neutron scattering [10]. This effect may be of great importance for the understanding of Alzheimer's disease, since a change in the mechanical properties of the lipid matrix could influence all membrane based signal cascades which are directly related to changes in protein and lipid mobility.

Acknowledgements

We thank the Helmholtz-Zentrum Berlin für Materialien und Energie for providing beamtime and technical support. Silvia

Seghezza is kindly acknowledged for her contribution to AFM imaging.

Appendix A. Supplementary data

Supplementary data to this article can be found online at doi:10.1016/j.bbamem.2011.07.024.

References

[1] D.J. Selkoe, The molecular pathology of Alzheimer's disease, Neuron 6 (1991) 487–498.
[2] D.M. Walsh, D.J. Selkoe, A beta oligomers — a decade of discovery, J. Neurochem. 101 (2007) 1172–1184.
[3] R. Cappai, A.R. White, Amyloid beta, Int. J. Biochem. Cell Biol. 31 (1999) 885–889.
[4] A. Demuro, E. Mina, R. Kayed, S.C. Milton, I. Parker, C.G. Glabe, Calcium dysregulation and membrane disruption as a ubiquitous neurotoxic mechanism of soluble amyloid oligomers, J. Biol. Chem. 280 (2005) 17294–17300.
[5] S. Dante, T. Hauss, A. Brandt, N.A. Dencher, Membrane fusogenic activity of the Alzheimer's peptide A beta(1–42) demonstrated by small-angle neutron scattering, J. Mol. Biol. 376 (2008) 393–404.
[6] C.M. Yip, A.A. Darabie, J. McLaurin, Abeta42-peptide assembly on lipid bilayers, J. Mol. Biol. 318 (2002) 97–107.
[7] S. Dante, T. Hauss, N.A. Dencher, beta-Amyloid 25 to 35 is intercalated in anionic and zwitterionic lipid membranes to different extents, Biophys. J. 83 (2002) 2610–2616.
[8] S. Dante, T. Hauss, N.A. Dencher, Insertion of externally administered amyloid beta peptide 25–35 and perturbation of lipid bilayers, Biochemistry-Us 42 (2003) 13667–13672.
[9] R.P. Mason, R.F. Jacob, M.F. Walter, P.E. Mason, N.A. Avdulov, S.V. Chochina, U. Igbavboa, W.G. Wood, Distribution and fluidizing action of soluble and aggregated amyloid β-peptide in rat synaptic plasma membranes, J. Biol. Chem. 274 (1999) 18801–18807.
[10] A. Buchsteiner, T. Hauss, S. Dante, N.A. Dencher, Alzheimer's disease amyloid-beta peptide analogue alters the ps-dynamics of phospholipid membranes, Biochim. Biophys. Acta-Biomembranes 1798 (2010) 1969–1976.
[11] J. Majewski, J.Y. Wong, C.K. Park, M. Seitz, J.N. Israelachvili, G.S. Smith, Structural studies of polymer-cushioned lipid bilayers, Biophys. J. 75 (1998) 2363–2367.
[12] J.Y. Wong, J. Majewski, M. Seitz, C.K. Park, J.N. Israelachvili, G.S. Smith, Polymer-cushioned bilayers. I. A structural study of various preparation methods using neutron reflectometry, Biophys. J. 77 (1999) 1445–1457.
[13] J.Y. Wong, C.K. Park, M. Seitz, J. Israelachvili, Polymer-cushioned bilayers. II. An investigation of interaction forces and fusion using the surface forces apparatus, Biophys. J. 77 (1999) 1458–1468.
[14] K. Jacobson, E.D. Sheets, R. Simson, Revisiting the fluid mosaic model of membranes, Science 268 (1995) 1441–1442.
[15] P.A. Janmey, C. Chaponnier, Medical aspects of the actin cytoskeleton, Curr. Opin. Cell Biol. 7 (1995) 111–117.
[16] G. Decher, Fuzzy nanoassemblies: toward layered polymeric multicomposites, Science 277 (1997) 1232–1237.
[17] T. Baumgart, M. Kreiter, H. Lauer, R. Naumann, G. Jung, A. Jonczyk, A. Offenhausser, W. Knoll, Fusion of small unilamellar vesicles onto laterally mixed self-assembled monolayers of thiolipopeptides, J. Colloid Interface Sci. 258 (2003) 298–309.
[18] E. Kalb, S. Frey, L.K. Tamm, Formation of supported planar bilayers by fusion of vesicles to supported phospholipid monolayers, Biochim. Biophys. Acta 1103 (1992) 307–316.
[19] G. Fragneto-Cusani, Neutron reflectivity at the solid/liquid interface: examples of applications in biophysics, J. Phys. Condens. Matter 13 (2001) 4973–4989.
[20] S. Krueger, Neutron reflection from interfaces with biological and biomimetic materials, Curr. Opin. Colloid Interface Sci. 6 (2001) 111–117.
[21] B. Klosgen, T. Spangenberg, H. Niehus, T. Gutberlet, R. Steitz, G. Fragneto, Membranes at interfaces: structure studies by AFM and time-resolved neutron reflectivity, Cell. Mol. Biol. Lett. 7 (2002) 240.
[22] F. Rehfeldt, R. Steitz, S.P. Armes, R. Von Klitzing, A.P. Gast, M. Tanaka, Reversible activation of diblock copolymer monolayers at the interface by pH modulation, 1: lateral chain density and conformation, J. Phys. Chem. B 110 (2006) 9171–9176.
[23] M. Canale, M. Milanese, C. Novara, Semi-active suspension control using "fast" model-predictive techniques, IEEE Trans. Control Syst. Technol. 14 (2006) 1034–1046.
[24] S. Chiantia, N. Kahya, P. Schwille, Raft domain reorganization driven by short- and long-chain ceramide: a combined AFM and FCS study, Langmuir 23 (2007) 7659–7665.
[25] C.M. Yip, J. McLaurin, Amyloid-beta peptide assembly: a critical step in fibrillogenesis and membrane disruption, Biophys. J. 80 (2001) 1359–1371.
[26] Y.F. Dufrene, W.R. Barger, J.B.D. Green, G.U. Lee, Nanometer-scale surface properties of mixed phospholipid monolayers and bilayers, Langmuir 13 (1997) 4779–4784.
[27] Y.F. Dufrene, W.R. Barger, G.U. Lee, Direct characterization of mixed phospholipid/glycolipid bilayers with chemically-functionalized AFM probes, Biophys. J. 74 (1998) A330–A.
[28] V. Franz, S. Loi, H. Muller, E. Bamberg, H.H. Butt, Tip penetration through lipid bilayers in atomic force microscopy, Colloids Surf. B Biointerfaces 23 (2002) 191–200.
[29] C. Canale, M. Jacono, A. Diaspro, S. Dante, Force spectroscopy as a tool to investigate solid supported lipid membranes, Microsc. Res. Tech. 73 (2010) 965–974.
[30] S. Jao, K. Ma, J. Talafous, R. Orlando, M.G. Zagorski, Trifluoroacetic acid pretreatment reproducibly disaggregates the amyloid β-peptide, Amyloid: Int. J. Exp. Clin. Invest. 4 (1997) 240–244.
[31] J.R. Howse, E. Manzanares-Papayanopoulos, I.A. McLure, J. Bowers, R. Steitz, G.H. Findenegg, Critical adsorption and boundary layer structure of 2-butoxyethanol + D_2O mixtures at a hydrophilic silica surface, J. Chem. Phys. 116 (2002) 7177–7188.
[32] G. Decher, J.D. Hong, Buildup of Ultrathin multilayer films by a self-assembly process 1. Consecutive adsorption of anionic and cationic bipolar amphiphiles on charged surfaces, Makromol. Chem. Macromol. Symp. 46 (1991) 321–327.
[33] C. Delajon, T. Gutberlet, R. Steitz, H. Mohwald, R. Krastev, Formation of poly, electrolyte multilayer architectures with embedded DMPC studied *in situ* by neutron reflectometry, Langmuir 21 (2005) 8509–8514.
[34] R. Steitz, V. Leiner, R. Siebrecht, R. von Klitzing, Influence of the ionic strength on the structure of polyelectrolyte films at the solid/liquid interface, Colloids Surf. A-Physicochem. Eng. Aspects 163 (2000) 63–70.
[35] J.E. Wong, H. Zastrow, W. Jaeger, R. von Klitzing, Specific ion versus electrostatic effects on the construction of polyelectrolyte multilayers, Langmuir 25 (2009) 14061–14070.
[36] E. Blomberg, E. Poptoshev, F. Caruso, Surface interactions during polyelectrolyte multilayer build-up. 2. The effect of ionic strength on the structure of preformed multilayers, Langmuir 22 (2006) 4153–4157.
[37] M. Fischlechner, Lipid layers on polyelectrolyte multilayer supports, Soft Matter 4 (2008) 2245–2258.
[38] A. Chenal, L. Prongidi-Fix, A. Perier, C. Aisenbrey, G. Vernier, S. Lambotte, M. Haertlein, M.T. Dauvergne, G. Fragneto, B. Bechinger, D. Gillet, V. Forge, M. Ferrand, Deciphering membrane insertion of the diphtheria toxin T domain by specular neutron reflectometry and solid-state NMR spectroscopy, J. Mol. Biol. 391 (2009) 872–883.
[39] R. Nussinov, F.T. Arce, H.B. Jang, S. Ramachandran, P.B. Landon, R. Lal, Polymorphism of amyloid beta peptide in different environments: implications for membrane insertion and pore formation, Soft Matter 7 (2011) 5267–5273.
[40] R. Nussinov, H. Jang, F.T. Arce, S. Ramachandran, R. Capone, R. Lal, beta-Barrel topology of Alzheimer's beta-amyloid ion channels, J. Mol. Biol. 404 (2010) 917–934.
[41] R.M. Murphy, Kinetics of amyloid formation and membrane interaction with amyloidogenic proteins, Biochim. Biophys. Acta 1768 (2007) 1923–1934.
[42] A. Choucair, M. Chakrapani, B. Chakravarthy, J. Katsaras, L.J. Johnston, Preferential accumulation of A beta(1–42) on gel phase domains of lipid bilayers: an AFM and fluorescence study, Biochim. Biophys. Acta-Biomembranes 1768 (2007) 146–154.
[43] G. Valincius, F. Heinrich, R. Budvytyte, D.J. Vanderah, D.J. McGillivray, Y. Sokolov, J.E. Hall, M. Losche, Soluble amyloid beta-oligomers affect dielectric membrane properties by bilayer insertion and domain formation: implications for cell toxicity, Biophys. J. 95 (2008) 4845–4861.
[44] B. Jacrot, The study of biological structures by neutron scattering from solution, Rep. Prog. Phys. 39 (1976) 911–953.
[45] T.L. Lin, J.M. Lin, U.S. Jeng, Z.H. Huang, Y.S. Huang, Aggregation structure of Alzheimer amyloid-beta(1–40) peptide with sodium dodecyl sulfate as revealed by small-angle X-ray and neutron scattering, Soft Matter 5 (2009) 3913–3919.
[46] S.W. Chiu, S. Subramaniam, E. Jakobsson, Simulation study of a gramicidin/lipid bilayer system in excess water and lipid. I. Structure of the molecular complex, Biophys. J. 76 (1999) 1929–1938.